OPEN

Molecular Psychiatry (2017) 22, 407–416

www.nature.com/mp

ORIGINAL ARTICLE

Novel osmotin inhibits SREBP2 via the AdipoR1/AMPK/SIRT1 pathway to improve Alzheimer's disease neuropathological deficits

SA Shah[1,3], GH Yoon[1,3], SS Chung[2], MN Abid[1], TH Kim[1], HY Lee[1] and MO Kim[1]

Extensive evidence has indicated that a high rate of cholesterol biogenesis and abnormal neuronal energy metabolism play key roles in Alzheimer's disease (AD) pathogenesis. Here, for we believe the first time, we used osmotin, a plant protein homolog of mammalian adiponectin, to determine its therapeutic efficacy in different AD models. Our results reveal that osmotin treatment modulated adiponectin receptor 1 (AdipoR1), significantly induced AMP-activated protein kinase (AMPK)/Sirtuin 1 (SIRT1) activation and reduced SREBP2 (sterol regulatory element-binding protein 2) expression in both *in vitro* and *in vivo* AD models and in Adipo$^{-/-}$ mice. Via the AdipoR1/AMPK/SIRT1/SREBP2 signaling pathway, osmotin significantly diminished amyloidogenic Aβ production, abundance and aggregation, accompanied by improved pre- and post-synaptic dysfunction, cognitive impairment, memory deficits and, most importantly, reversed the suppression of long-term potentiation in AD mice. Interestingly, AdipoR1, AMPK and SIRT1 silencing not only abolished osmotin capability but also further enhanced AD pathology by increasing SREBP2, amyloid precursor protein (APP) and β-secretase (BACE1) expression and the levels of toxic Aβ production. However, the opposite was true for SREBP2 when silenced using small interfering RNA in APPswe/ind-transfected SH-SY5Y cells. Similarly, osmotin treatment also enhanced the non-amyloidogenic pathway by activating the α-secretase gene that is, *ADAM10*, in an AMPK/SIRT1-dependent manner. These results suggest that osmotin or osmotin-based therapeutic agents might be potential candidates for AD treatment.

Molecular Psychiatry (2017) **22,** 407–416; doi:10.1038/mp.2016.23; published online 22 March 2016

INTRODUCTION

Alzheimer's disease (AD) is marked by the accumulation of intracellular tangles of insoluble hyperphosphorylated tau proteins and abnormal protein deposits, or plaques, composed of amyloid-β (Aβ) peptides ($Aβ_{1–40}$ and $Aβ_{1–42}$) between neurons. These hallmarks are evident from the earliest stages of the disease, even before symptoms of memory loss and impaired learning are manifested. As AD progresses, memory loss and learning deficits increase as larger areas of the brain become affected by these tangles and plaques. Late-stage severe AD is characterized by extensive neurodegeneration, neuronal death and shrinkage of the brain. Cholesterol homeostasis is impaired in AD. There are several reports of an increased sterol burden in senile plaques in AD brains of humans and rodent models.[1–5] Both *in vitro* and *in vivo* studies have shown that high levels of serum cholesterol result in Aβ generation and therefore accelerate the progression of AD-like pathologies.[6]

AMP-activated protein kinase (AMPK) is an important energy sensor responsible for the maintenance of cellular energy homeostasis.[7] When cellular energy is depleted by stress, starvation, hypoxia or other means, AMPK is activated allosterically by the phosphorylation of its α-subunit on Thr-172 by upstream kinases following an increase in intracellular AMP.[8] Activated AMPK phosphorylates downstream targets, resulting in the inhibition of anabolic energy-consuming pathways (fatty acid and protein synthesis) and the stimulation of energy-producing catabolic pathways (such as fatty acid oxidation and glucose transport) to restore cellular energy homeostasis. Sirtuins are NAD^+-dependent protein deacetylases that sense elevated NAD^+ levels in response to changes in nutrient availability or stress and regulate the expression of genes involved in energy metabolism and the stress response. Of the seven mammalian sirtuins, sirtuin 1 (SIRT1) is the best characterized. AMPK and SIRT1 positively regulate each other's activities,[9] allowing them to coordinate their effects on energy metabolism.

The mammalian hormone adiponectin controls energy metabolism through the AMPK/SIRT1 pathway in skeletal muscle and liver.[10] Osmotin is a tobacco protein that is structurally and functionally similar to mammalian adiponectin, and its primary role in plants seems to involve defense against pathogens.[11] We recently reported that osmotin protected against Aβ-induced memory impairment, synaptic dysfunction and neurodegeneration in mice and also showed protection in the developing rodent brain against glutamate- and ethanol-induced neurodegeneration.[12–14] Here, we report for the first time that osmotin treatment reduces cholesterol biosynthesis pathways and ameliorates the progression of Alzheimer's disease pathologies and behavioral deficits in transgenic mice and *in vitro* AD models. In addition, we show that osmotin may exert its beneficial effects via the AdipoR1/AMPK/SIRT1/SREBP2 pathways in both Adipo$^{-/-}$ and amyloid precursor protein/presenilin 1 (APP/PS1) mice and in neuronal cell lines.

[1]Division of Life Science and Applied Life Science (BK21 Plus), College of Natural Sciences, Gyeongsang National University, Jinju, Republic of Korea and [2]Department of Physiology, College of Medicine, Yonsei University, Seoul, Republic of Korea. Correspondence: Professor MO Kim, Neuroscience Pioneer Research Center, Department of Biology, College of Natural Sciences, Gyeongsang National University, Jinju 660-701, Republic of Korea.
E-mail: mokim@gnu.ac.kr
[3]These two authors contributed equally to this work.
Received 4 September 2015; revised 2 February 2016; accepted 4 February 2016; published online 22 March 2016

MATERIALS AND METHODS

Most parts of this section are provided in the Supplementary Information.[15–18]

Mouse strains

Male Adipo$^{-/-}$ and congenic double-transgenic B6.Cg-Tg (APPswe, PSENdE9)85Dbo/Mmjax AD model mice were purchased from The Jackson Laboratory (Bar Harbor, ME, USA). The double-transgenic mice express a chimeric mouse–human amyloid precursor protein bearing the Swedish mutation (Mo/HuAPP695swe) and a mutant human Presenilin 1 protein (PS1-dE9) in central nervous system neurons. Transgenic C57BL/6J-Tg (NSE-APPsw) KLAR mice, which overexpress a mutant form of the human amyloid precursor protein bearing the Swedish (K670N/M671L) mutation from the neuron-specific enolase promoter, were obtained from the Ministry of Food and Drug Safety (Cheongju, Republic of Korea). Male C57BL/6J mice (wild type (WT)) were purchased from Samtako Bio (Osan, Republic of Korea). Mice were housed under a 12 h light/12 h dark cycle at 25 °C with *ad libitum* access to food and water. The experimental procedures were approved by the animal ethics committee of the Department of Applied Life Sciences at Gyeongsang National University, Republic of Korea.

Osmotin treatment details in mice

Mice were grouped before treatment as follows: WT mice were randomly divided into two groups: saline treated and osmotin treated. Transgenic mice (single and double) were randomly divided into three subgroups: (1) saline treated; (2) osmotin treated for a short period (12 μg per g of body weight) two times (two consecutive days); and (3) osmotin treated for a long period (5 μg per g of body weight) 2 times per week for 2 weeks and 4 weeks respectively. Similarly, 3-month-old male Adipo$^{-/-}$ mice were divided into two groups, that is, vehicle-treated Adipo$^{-/-}$ and osmotin-treated Adipo$^{-/-}$ for 2 weeks. Osmotin in saline solution was administered via intraperitoneal injection. Mice were decapitated at the age of 5, 9, 12 or 16 months.

Statistical analysis

For western blots, densities of values are expressed as the mean ± s.e.m. with arbitrary units. Prism 5 (GraphPad Software, San Diego, CA, USA) was used for one-way analysis of variance (ANOVA) followed by Student's *t*-test for data from the western and morphological analyses and enzyme-linked immunosorbent assays. One-way ANOVA with *post hoc* Tukey's test was used to analyze the electrophysiological data. The escape latency data were analyzed using ANOVA with training days as repeated measurements. For the probe tests, statistical comparisons between groups for the time over quadrants were performed using one-way ANOVA. The data were considered significant at $P < 0.05$, 0.01 and 0.001.

RESULTS

Osmotin suppressed the toxic effects of $A\beta_{1-42}$ in a neuronal cell line

First, the neuroprotective effects of osmotin against $A\beta_{1-42}$-induced toxicity in human neuroblastoma SH-SY5Y cells were examined using an ApoTox-Glo Triplex Assay (Supplementary Figures S1a–c). The results of the viability assay indicated that $A\beta_{1-42}$ caused a significant decrease in cell viability, whereas three concentrations of osmotin (0.1, 0.2 and 0.4 μM) alone were nontoxic to the cells. In combination with $A\beta_{1-42}$, all three concentrations of osmotin significantly increased cell viability. Similarly, the $A\beta_{1-42}$ treatment increased cytotoxicity and caspase3/7 levels compared with an untreated control, whereas osmotin (0.1, 0.2 and/or 0.4 μM) had no significant effects. When applied as cotreatment with $A\beta_{1-42}$, osmotin significantly ($P < 0.001$) suppressed the effects of $A\beta_{1-42}$ on cytotoxicity and caspase3/7 levels (Supplementary Figures S1a–c).

Osmotin modulated AdipoR1 and reduced Aβ via the AMPK/SIRT1/SREBP2 pathway

We investigated the modulatory effect of osmotin on adiponectin receptor 1 (AdipoR1) *in vitro* in APPswe/ind-transfected human neuroblastoma SH-SY5Y cells treated with osmotin in the presence or absence of AdipoR1 (small interfering RNA (siRNA) silenced). We observed a lower expression of AdipoR1 in the APP-transfected cells compared with the untreated control, and osmotin treatment positively modulated the expression of AdipoR1, whereas AdipoR1 expression further decreased when it was silenced using AdipoR1 siRNA; furthermore, osmotin was unable to increase its expression in APP-transfected cells (Supplementary Figure S1d). In addition, osmotin treatment significantly activated AMPK and SIRT1 and inhibited SREBP2 (sterol-regulatory element-binding protein 2) and Aβ protein expression in APP-transfected SH-SY5Y cells. Interestingly, AdipoR1 silencing further reduced AMPK and SIRT1 along with significantly increasing SREBP2 and Aβ expression. Most importantly, AdipoR1 silencing abolished the ability of osmotin to activate the AMPK and SIRT1 proteins and to inhibit the SREBP2 and Aβ proteins (Supplementary Figure S1d).

We next analyzed AdipoR1 expression in brain homogenates from 9- and 12-month-old APP/PS1 mice and 3-month-old Adipo$^{-/-}$ mice treated with either vehicle or osmotin. The immunoblot results indicated lower expression of AdipoR1 in both the 9- and 12-month-old APP/PS1 double-transgenic mice and in the 3-month-old Adipo$^{-/-}$ mice, whereas osmotin increased the expression of AdipoR1 in WT and AD mice of both ages and in Adipo$^{-/-}$ mice (Supplementary Figures S1e and f).

Osmotin induced the activation of AMPK and SIRT1 in both *in vitro* and *in vivo* models

We then studied the expression of activated AMPK (p-AMPKα (Thr^{172})) and SIRT1 because they are both cellular energy-sensing enzymes. We either treated SH-SY5Y cells with $A\beta_{1-42}$ (5 μM) or transfected them with APPswe/ind and added osmotin (0.2 μM) for 24 h. Both the Aβ treatment (Figure 1a) and APP transfection (Figures 1d–f) of these cells resulted in the suppression of p-AMPK and SIRT1 protein expression and activity (Figures 1b and c), whereas 0.2 μM osmotin treatment reversed these changes (Figures 1a–f). Interestingly, the protective effects of osmotin against the Aβ or APP transfection-induced suppression of p-AMPK and SIRT1 expression levels and activities could be abolished by cotreatment with either an AMPK inhibitor, that is, compound C (20 μM), or the silencing of AMPK with siRNA and a SIRT1 inhibitor, that is, EX527 (80 μM), or SIRT1 siRNA, respectively, indicating that the observed protection was not an artifact (Figures 1a–f). Similarly, we showed that both AMPK and SIRT1 were dependent on each other because they were both silenced by their respective siRNAs in APP-transfected SH-SY5Y cells (Figure 1f).

In addition, the levels of p-AMPKα and SIRT1 were lower in the hippocampi of Adipo$^{-/-}$ mice and APP/PS1 (5-, 9- and 12-month-old) and APP_{SW} (12-month-old) mice compared with WT mice (Figure 1g and Supplementary Figure S1e). Accordingly, the activities of AMPK and SIRT1 were also lower in brain tissues of Adipo$^{-/-}$ mice and APP/PS1 mice (Figure 1h). Osmotin treatment for a short period of time increased the p-AMPKα and SIRT1 levels in the hippocampi of 5-, 9- and 12-month-old APP/PS1 and 12-month-old APP_{SW} mice (Figure 1g). In agreement with these results, we also observed increases in the activities of AMPK and SIRT1 in brain homogenates of osmotin-treated APP/PS1 mice and Adipo$^{-/-}$ mice compared with the respective vehicle-treated mice (Figure 1h). Similarly, osmotin administration over a long period of time (2 and 4 weeks) also increased the p-AMPKα and SIRT1 levels compared with vehicle-treated APP/PS1 mice and Adipo$^{-/-}$ mice, respectively (Supplementary Figures S1d and e).

Osmotin reduced Aβ production and aggregation by negatively regulating the levels of cholesterol and SREBP2 *in vivo*

We first examined the total cholesterol, low-density lipoprotein cholesterol, high-density lipoprotein cholesterol, free fatty acid and triglyceride levels in the sera of osmotin-treated and

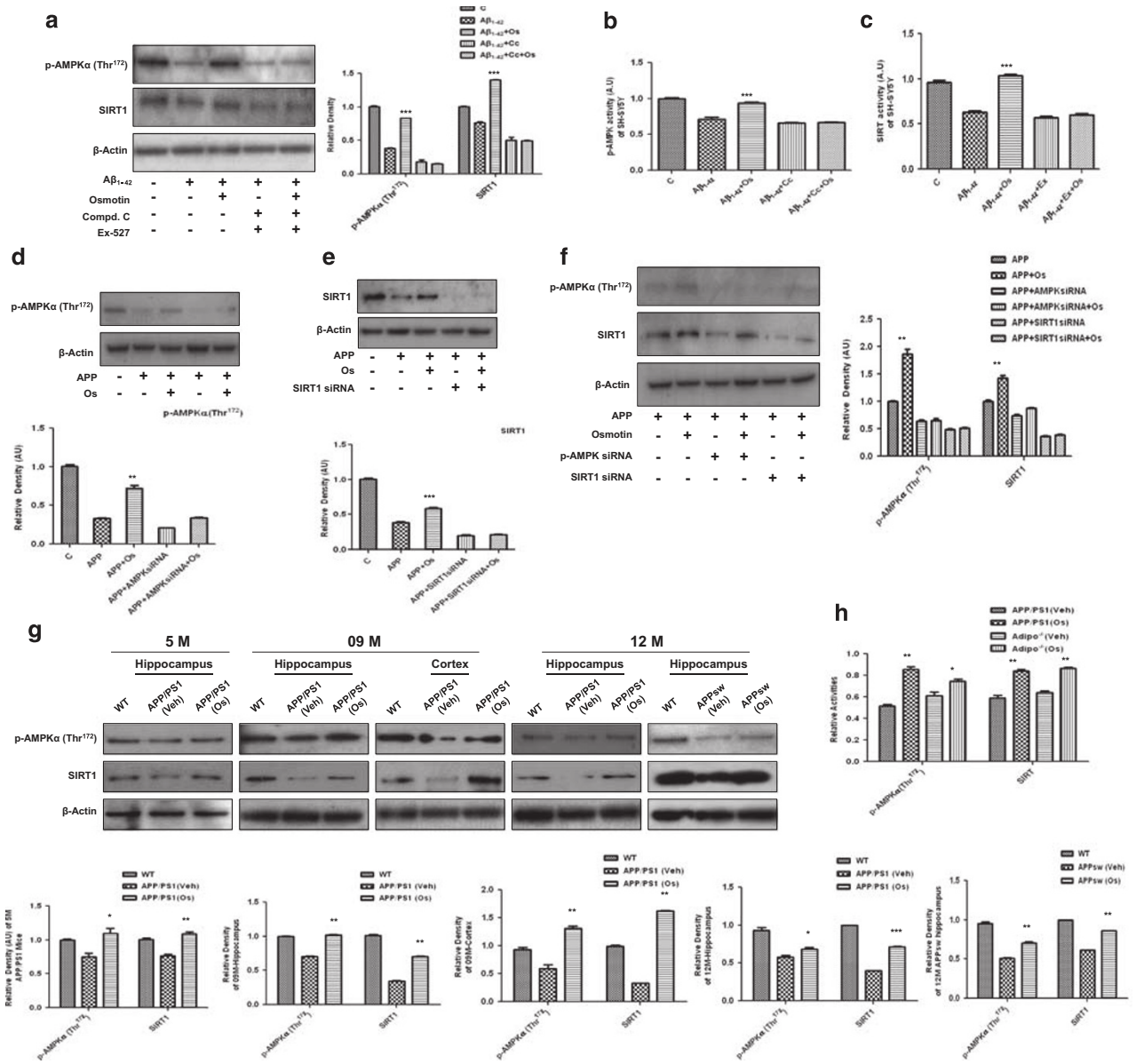

Figure 1. Osmotin increased phosphorylated AMP-activated protein kinase (p-AMPK) and sirtuin 1 (SIRT1) levels and their activities *in vitro* and *in vivo*. (**a**) Western blot analysis of p-AMPK and SIRT1 in lysates of SH-SY5Y cells after treatment with $A\beta_{1-42}$ (5 μM), osmotin (Os; 0.2 μM), compound C (C; 20 μM) and EX527 (80 μM) for 24 h and (**b**, **c**) their activity histograms. (**d–f**) Western blot analysis with the respective density histograms of p-AMPK and SIRT1 in lysates of APPswe/ind-transfected (for 72 h) SH-SY5Y cells subjected to the small interfering RNA (siRNA)-induced silencing of AMPK and SIRT1 for 48 h, respectively, after 24 h of treatment with Os (0.2 μM). (**g**) Western blot analyses of p-AMPK and SIRT1 levels in hippocampal extracts from 5-, 9- and 12-month-old wild-type (WT) and vehicle (Veh)- or Os-treated (for a short time) amyloid precursor protein/presenilin 1 (APP/PS1) and APP_{SW} mice and (**h**) AMPK and SIRT activity histograms in brain homogenates of $Adipo^{-/-}$ and APP/PS1 mice. The assays were performed three times with similar results, and representative data from one experiment with triplicate samples are shown. The bands were quantified using Sigma Gel System (SPSS, Chicago, IL, USA), and their differences are presented as histograms derived from a one-way analysis of variance (ANOVA) followed by a *t*-test and as the mean ± s.e.m. for the respective indicated proteins ($n = 5$/group). After developing of respective antibodies, membranes were reprobed for the β-actin signal, shown as the loading control. Histograms depict analyses of band density relative to the density of WT on the same blot. Significance: $^*P < 0.05$, $^{**}P < 0.01$ and $^{***}P < 0.001$.

vehicle-treated APP/PS1 and $Adipo^{-/-}$ mice to determine the effects of osmotin on cholesterol levels in these mouse strains (Supplementary Figure S2a). Our results indicated that osmotin treatment significantly reduced the total cholesterol, low-density lipoprotein cholesterol, free fatty acid and triglyceride levels and increased the high-density lipoprotein level compared with the vehicle-treated APP/PS1 and $Adipo^{-/-}$ mice (Supplementary Figure S2a).

Next, we performed western blotting to determine the cellular levels of SREBP2 in the brains of APP/PS1 and $Adipo^{-/-}$ mice. We showed that compared with WT mice, the levels of SREBP2 were higher in the hippocampi of vehicle-treated $Adipo^{-/-}$ mice and APP/PS1 mice at the ages of 5, 9 and 12 months. Osmotin treatment reduced the levels of SREBP2 in the brain tissues of $Adipo^{-/-}$ mice and APP/PS1 mice of all ages (5–12 months old) compared with the vehicle-treated mice (Figure 2a and Supplementary Figure S2b).

After negatively regulating the cholesterol level, we performed different techniques to determine whether osmotin affects the amyloidogenic pathway of Aβ production and deposition in

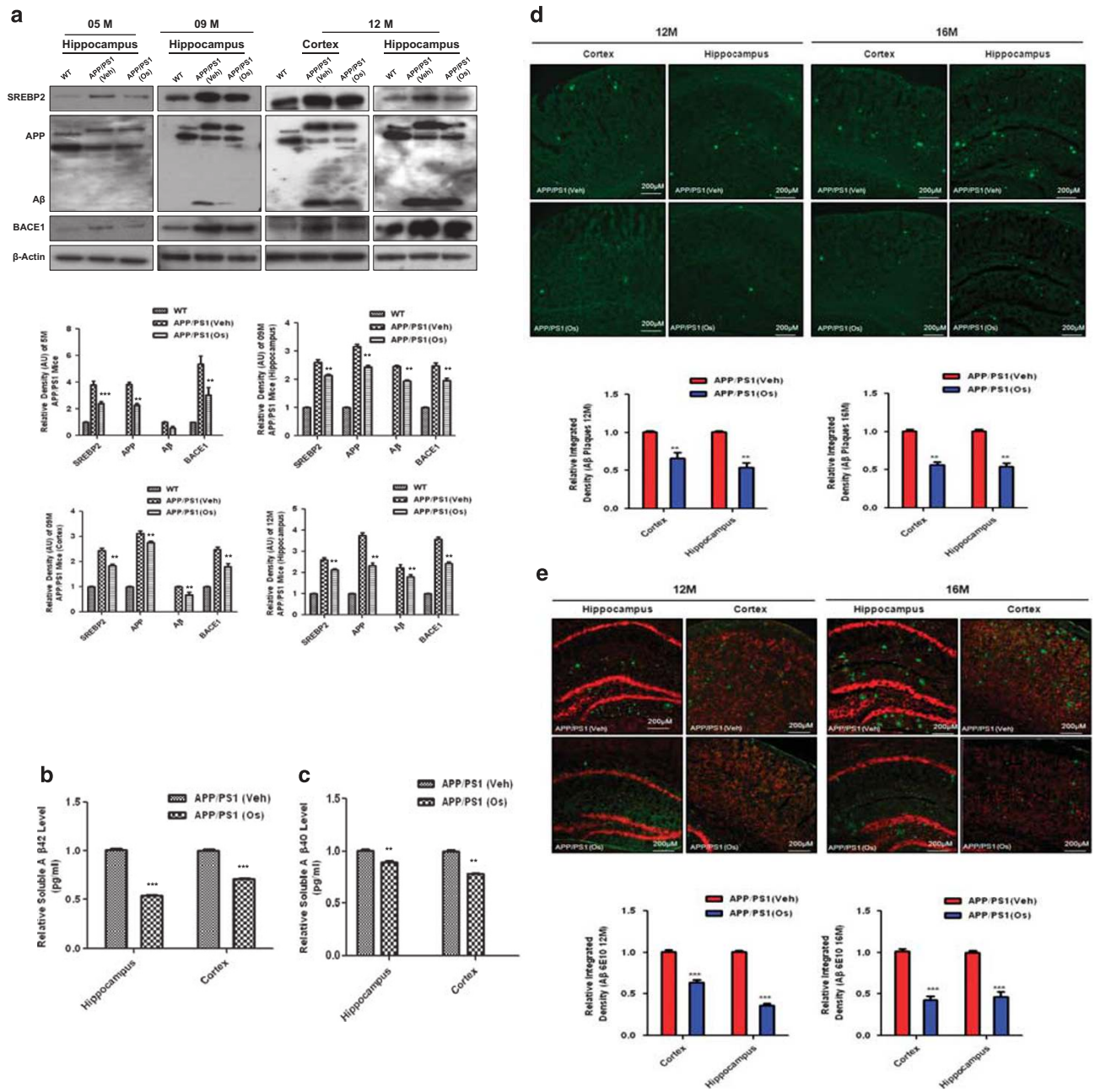

Figure 2. Osmotin reduced amyloid burden by inhibiting SREBP2 (sterol regulatory element-binding protein 2) expression in amyloid precursor protein/presenilin 1 (APP/PS1) mice. (**a**) Western blot analysis of SREBP2, BACE1, APP and amyloid-β (Aβ) levels in hippocampal and cortex extracts from 5-, 9- and 12-month-old wild-type (WT) and vehicle (Veh)- or osmotin (Os)-treated (for a short time) APP/PS1 mice. Representative blots and histograms depicting analyses of band density relative to WT bands are shown. The membranes were reprobed for β-actin as a housekeeping control. The bars indicate the mean ± s.e.m. ($n = 5$/group). (**b**, **c**) Enzyme-linked immunosorbent assay (ELISA) histograms (relative) of soluble (**b**) $A\beta_{1-42}$ and (**c**) $A\beta_{1-40}$ in cortex and hippocampal brain homogenates of APP/PS1 mice with or without osmotin treatment. All of the methods and procedures recommended by the manufacturer were followed, and experiments were performed in triplicate. (**d**, **e**) Fluorescence images with relative density histograms of cortex and hippocampal regions of 12- and 16-month-old Veh- and Os-treated (4 weeks) APP/PS1 mice, indicating the localization of (**d**) Aβ plaques and (**e**) Aβ (6E10) aggregates. Significance: $^{*}P < 0.05$, $^{**}P < 0.01$ and $^{***}P < 0.001$.

APP/PS1 mice of different ages. Western blot analysis of protein extracts showed that the levels of APP, the amyloidogenic β-secretase BACE1 and Aβ were higher in the brain tissues of vehicle-treated APP/PS1 mice of different ages, including 5-, 9- and 12-month-old mice. Conversely, osmotin administration significantly lowered the levels of these proteins, as shown in the results obtained using brain tissues from APP/PS1 mice (Figure 2a). The levels of soluble $A\beta_{1-42}$ and $A\beta_{1-40}$ were measured using enzyme-linked immunosorbent assay in brain homogenates of transgenic mice after osmotin treatment, and the results indicated that osmotin treatment significantly reduced the levels of soluble $A\beta_{1-42}$ and $A\beta_{1-40}$ in the hippocampi and cortices of APP/PS1 mice (Figures 2b and c).

In addition, we performed thioflavin S and Aβ antibody (6E10) immunostaining to examine both 12- and 16-month-old APP/PS1 mouse brains after osmotin administration for 4 weeks. The results

indicated that osmotin significantly reduced the amounts of Aβ aggregation and deposition in the cortices and hippocampi of APP/PS1 mice after osmotin administration for 4 weeks (Figures 2d and e).

Osmotin reduced the amyloidogenic pathway of Aβ production in an AMPK/SIRT1/SREBP2-dependent manner *in vitro*

To examine the detailed mechanism of osmotin reduction via the amyloidogenic pathway, we transfected SH-SY5Y cells with APPswe/ind for 72 h. The results indicated that osmotin treatment for 24 h significantly reduced the expression of APP and Aβ in APPswe/ind-transfected SH-SY5Y cells. Interestingly, when both AMPK and SIRT1 were silenced with their respective siRNAs, the APP and Aβ levels were further significantly increased, and osmotin was unable to reduce their expression levels (Figure 3a). In accordance with these findings, the APP level was also increased in cells containing AMPK siRNA, but it was dramatically decreased in cells containing SREBP2 siRNA (Figure 3b).

In addition, we assessed the expression of BACE1 and SREBP2 in APPswe/ind-transfected SH-SY5Y cells. It was evident from the blot results that the expression levels of both BACE1 and SREBP2 in cell lysates were increased as a result of APP transfection; however, when AMPK was silenced by siRNA, the expression levels of both BACE1 and SREBP2 further increased, and the suppressive ability of osmotin was abolished (Figure 3c). We then silenced SREBP2 with siRNA and measured the BACE1 and SREBP2 levels in APP-transfected SH-SY5Y cells. The results indicated that after APP transfection, the expression levels of both BACE1 and SREBP2 were significantly higher compared with the control, and when SREBP2 was silenced by siRNA, the expression levels of BACE1 and SREBP2 were dramatically decreased (Figure 3d).

Osmotin enhanced the non-amyloidogenic gene *ADAM10* in an AMPK/SIRT1-dependent manner both *in vivo* and *in vitro*

Similarly, the protein levels of sAPP-α, ADAM10 and ADAM17 were lower in the brain tissues of vehicle-treated APP/PS1 mice compared with WT mice. The levels of sAPP-α and the α-secretases ADAM10 and ADAM17 were significantly higher in the brain tissues of osmotin-treated APP/PS1 mice compared with vehicle-treated controls (Figure 3e). To determine whether the beneficial effect of osmotin on the non-amyloidogenic pathway is also AMPK and SIRT1 dependent, we measured ADAM10 levels in APP-transfected SH-SY5Y cells and in cells following AMPK and SIRT1 siRNA-induced silencing. The results indicated that the expression of ADAM10 was decreased in APP-transfected cells and was enhanced by osmotin; however, when AMPK and SIRT1 were silenced with their respective siRNAs, ADAM10 expression was further dramatically decreased, and the suppressive ability of osmotin was also blocked (Figures 3f–h), indicating that the neuroprotective functions of osmotin may be mediated by AMPK and SIRT1 (Figures 3f–h).

Osmotin protected against the loss of NMDA receptors and NMDAR activity in APP/PS1 mice

The expression levels of both *N*-methyl-D-aspartate receptors NMDAR1 (NR1) and NMDAR2 (NR2), which control synaptic plasticity, synapse formation and memory function, were measured with western blotting. Reduced levels of NR1 and NR2 were observed in the brain tissues of vehicle-treated APP/PS1 mice, whereas osmotin treatment increased the levels in the brain tissues of APP/PS1 mice (Supplementary Figures S3a and b). A previous study has reported that synaptosomal-associated protein of 23 kDa (SNAP-23) and SNAP-25 are important for the trafficking of NMDARs to the cell surface. Western blot analysis of tissue extracts (Supplementary Figure S3a) and immunofluorescence analyses of tissue sections (Supplementary Figure S3b) confirmed that the levels of SNAP23, SNAP25, synaptophysin and PSD95 in the hippocampi and cortices of the brains of vehicle-treated APP/PS1 mice were lower than those in the hippocampi and cortices of the brains of WT mice and that osmotin treatment protected the APP/PS1 mice against these decreases (Supplementary Figures S3a and b). In the hippocampus, these trends for synaptophysin and SNAP23 were observed in the dentate gyrus and CA1 regions.

Osmotin augmented the number of functional synapses without affecting synaptic strength and rescued LTP deficits in AD models

To investigate whether osmotin has an effect on the plasticity of functional synapses, we measured α-amino-3-hydroxy-5-methyl-4-isoxazolepropionic acid (AMPA) receptor-mediated miniature excitatory postsynaptic currents (mEPSCs) in cultured hippocampal cells at 21 days *in vitro* following 24 h of treatment with osmotin (8 to 32 nM) or vehicle. Osmotin (16 and 32 nM) significantly increased the mean frequency of mEPSCs compared with vehicle-treated controls. However, osmotin treatment had little effect on the mean amplitudes of AMPAR-mediated mEPSCs in all osmotin-treated groups, suggesting that this treatment did not induce alterations in postsynaptic strength (Supplementary Figure S4a1). Next, to investigate the effects of osmotin on synaptic function under Alzheimer's disease-like pathological conditions, we measured AMPAR-mediated mEPSCs in hippocampal cells at 21 days *in vitro* following 24 h of treatment with vehicle, $A\beta_{1-42}$ (0.05 μg ml^{-1}) or $A\beta_{1-42}$ (0.05 μg ml^{-1}) plus osmotin (32 nM). As reported previously, Aβ significantly decreased the mean frequency of AMPAR-mediated mEPSCs compared with the vehicle-treated control, whereas osmotin (32 nM) reversed the effects of Aβ (Supplementary Figure S4b1). Moreover, there were no significant differences in mean mEPSC amplitudes between the vehicle group and the Aβ or Aβ plus osmotin groups, indicating that these treatments did not induce significant alterations in postsynaptic strength.

To investigate the effect of osmotin on the plasticity of functional synapses in an *ex vivo* preparation, we measured AMPA-mediated mEPSCs in the hippocampal CA1 region in acute slices prepared from WT, vehicle-treated transgenic AD (APP/PS1) and osmotin-treated APP/PS1 mice. As shown in Figure 4a1 and 3, the mean frequency of mEPSCs was significantly reduced in the APP/PS1 mice compared with the WT mice, as expected. Surprisingly, osmotin significantly reversed the reduction in AMPA-mediated mEPSCs almost to the level observed in the WT mice (14.4 ± 2.0 Hz, $n = 7$ for WT; 7.5 ± 1.0 Hz, $n = 6$ for APP/PS1+vehicle; 13.91 ± 1.3 Hz, $n = 6$ for APP/PS1+osmotin; one-way ANOVA with *post hoc* Tukey's test, WT versus APP/PS1+vehicle, $P < 0.05$; APP/PS1+vehicle versus APP/PS1+osmotin, $P < 0.05$) (Figure 4a3). However, osmotin treatment had little effect on the mean amplitude of AMPA-mediated mEPSCs in all the osmotin-treated groups, suggesting that there were no postsynaptic alterations in synaptic strength (4.4 ± 0.3 pA, $n = 7$ for WT; 4.9 ± 0.2 pA, $n = 6$ for APP/PS1 +vehicle; 4.5 ± 0.2 pA, $n = 6$ for APP/PS1+osmotin; one-way ANOVA, $P > 0.05$) (Figure 4a2 and 3).

In addition, we investigated whether the improvement in cognitive performance following osmotin treatment was associated with the modulation of synaptic function and plasticity. To this end, we performed electrophysiology experiments using acute hippocampal slices prepared from WT, vehicle-treated transgenic AD (APP/PS1) and osmotin-treated APP/PS1 mice. At Schaffer collateral inputs to CA1, long-term potentiation (LTP) was significantly suppressed in the hippocampal CA1 regions of APP/PS1 mice compared with WT mice (Figure 4b1 and 2). Surprisingly, osmotin reversed the suppressed LTP responses in the hippocampal CA1 regions of APP/PS1 mice, increasing them to the WT level (92.0 ± 9.6% increase, $n = 3$ for WT; 32.0 ± 8.5%

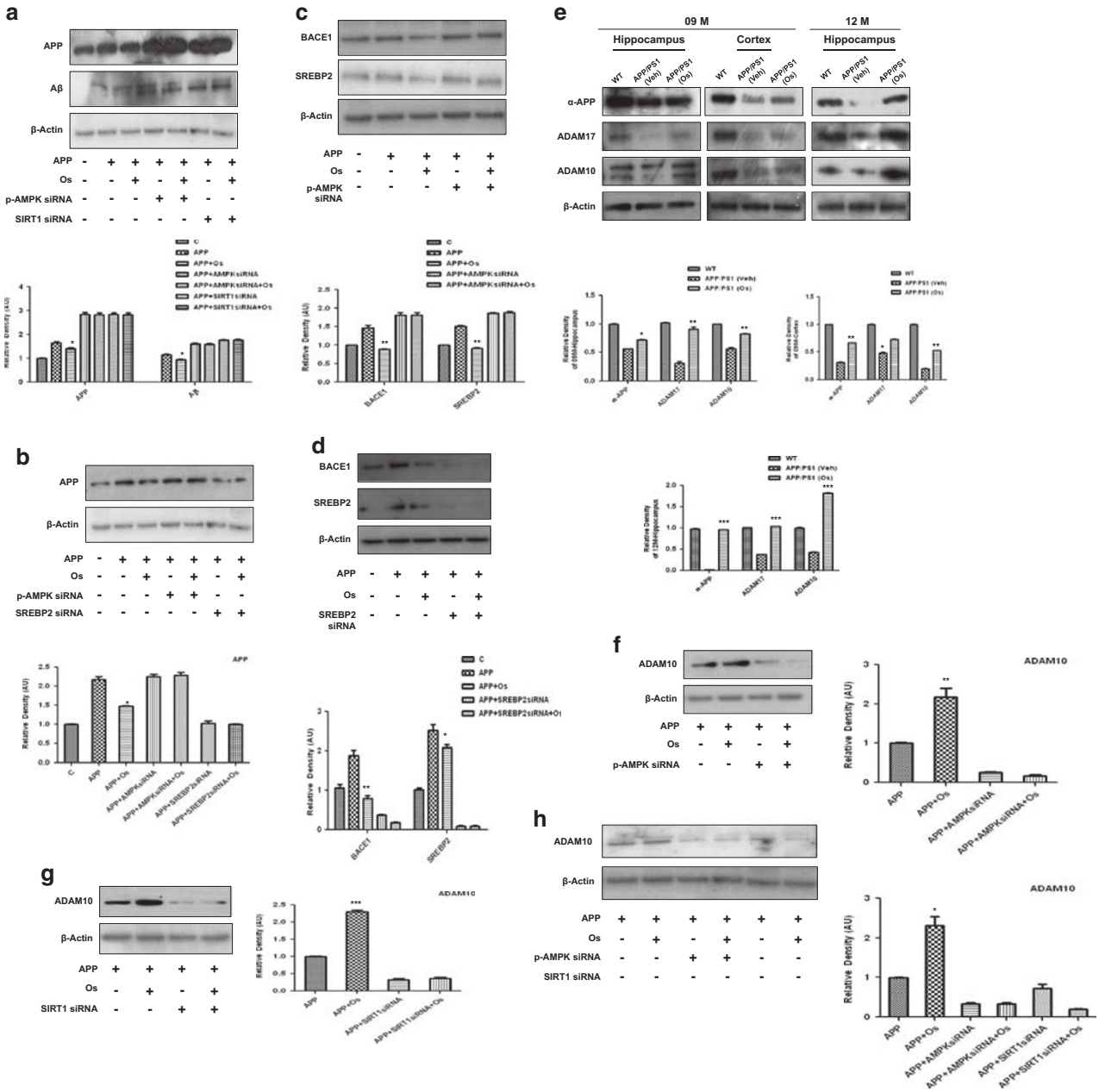

Figure 3. Osmotin (Os) reduced amyloid-β (Aβ) production in APPswe/ind-transfected SH-SY5Y cells in an AMPK/SIRT1/SREBP2-dependent manner. Western blot analysis and respective density histograms of (**a**) amyloid precursor protein (APP) and Aβ, (**b**) APP and (**c**, **d**) BACE1 and SREBP2 (sterol regulatory element-binding protein 2) in APPswe/ind-transfected SH-SY5Y cells subjected to the small interfering RNA (siRNA)-induced silencing of AMP-activated protein kinase (AMPK), sirtuin 1 (SIRT1) and SREBP2, respectively. Cells were transfected for 72 h followed by siRNA treatment for 48 h and osmotin treatment for 24 h. The β-actin signal is shown as a loading control. (**e**) Osmotin treatment increased the levels of sAPP-α, ADAM10 and ADAM17 protein expression in brain tissues homogenates from 9-month-old APP/presenilin 1 (PS1) mice compared with vehicle-treated mice. (**f–h**) ADAM10 western blot analyses and respective density histograms of APPswe/ind-transfected SH-SY5Y cells subjected to the siRNA-induced silencing of AMPK and SIRT1. All the respective details are described in the Materials and methods section. Significance: $^{*}P < 0.05$, $^{**}P < 0.01$ and $^{***}P < 0.001$.

increase, $n = 4$ for APP/PS1+vehicle; 85.0 ± 15.4% increase, $n = 4$ for APP/PS1+osmotin; one-way ANOVA with *post hoc* Tukey's test; WT versus APP/PS1+vehicle, $P < 0.05$; APP/PS1+vehicle versus APP/PS1+osmotin, $P < 0.05$) (Figure 4b3 and 4). These data suggest that osmotin treatment restored synaptic plasticity and the number of functional synapses, which are significantly deteriorated in AD, implying a role for osmotin in improving memory and cognition.

Osmotin protected against memory and cognitive deficits in APP and APP/PS1 mice

Finally, we examined the effects of osmotin on hippocampal-dependent memory and cognition in single (APP) and double-transgenic (APP/PS1) mice using the MWM and Y-maze tasks. During the session before treatment, the escape latency from the water to the submerged platform was significantly higher for all of the animals, including the WT and transgenic APP and APP/PS1

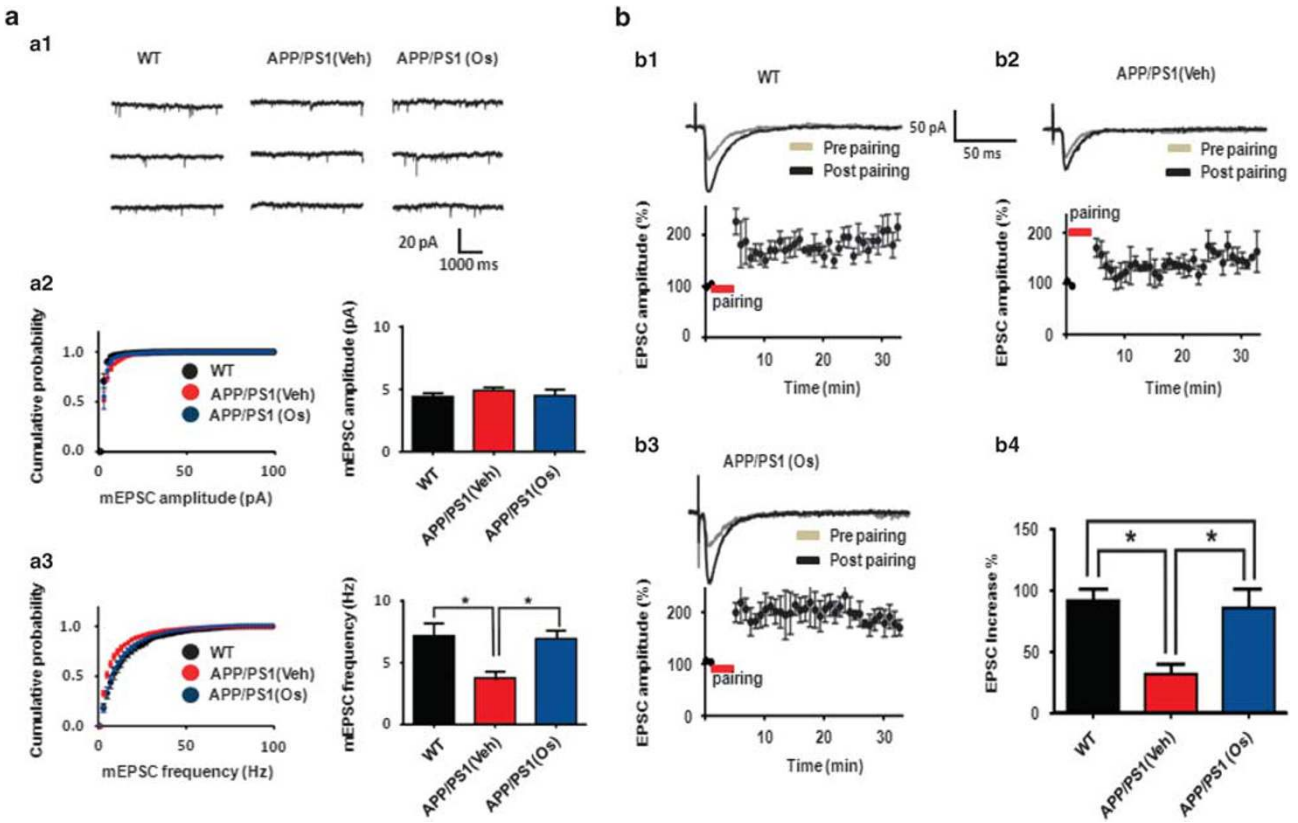

Figure 4. Osmotin (Os) augmented the number of functional synapses without affecting synaptic strength and rescued long-term potentiation (LTP) deficits in the CA1 region of hippocampal slices from Alzheimer's disease (AD) mice. (**aa**1) Representative traces of spontaneous unitary excitatory postsynaptic currents (EPSCs) recorded in the CA1 region of hippocampal slices from wild-type (WT; left trace), amyloid precursor protein/presenilin 1 (APP/PS1) and osmotin-treated APP/PS1 (right trace) mice. (**a**2, left) Cumulative miniature EPSC (mEPSC) amplitude distributions from all recorded neurons for the three mouse groups (control (black circle), APP/PS1 (red trace) and osmotin-treated APP/PS1 (blue circle) groups). (**a**2, right) Summary of mEPSC amplitudes for the three groups. (**a**3, left) Cumulative mEPSC frequency distributions from all recorded neurons for the three groups. (**a**3, right) Summary of mEPSC amplitudes for the three groups. Summary of mEPSC frequencies in control APP/PS1 and osmotin-treated APP/PS1 mice. (**b**1, 2, 3, upper trace) A representative trace of LTP induction in the CA1 region of the hippocampi of control mice, APP/PS1 mice and osmotin-treated APP/PS1 mice, respectively. (**b**1, 2, 3, lower trace) Average time course of LTP induction in the CA1 region of the hippocampi of control, APP/PS1 mice and osmotin-treated APP/PS1 mice, respectively. (**b**4) Summary of the effects of osmotin on LTP induction in APP/PS1 mice. The bars represent the mean ± s.e.m. ($n = 8$). Significance: $^*P < 0.05$.

mice, compared with day 1 of treatment, whereas the WT mice learned the task quickly, as shown by a sharp decrease in escape latency. However, the APP and APP/PS1 mice showed learning deficits on days 2 and 3 that were consistent with the reported spatial learning and memory deficits in APP/PS1 mice, as shown in Figure 5a and Supplementary Figure S5a.

The administration of osmotin to the APP and APP/PS1 mice resulted in a significant reduction in the mean escape latency time compared with the untreated mice. The histograms show that the decrease in the mean escape latency started on day 1 and continued until days 3 and 7 for the APP and APP/PS1 mice, respectively, and was persistent compared with the vehicle-treated APP and APP/PS1 mice (Figure 5b and Supplementary Figure S5a). The mice were allowed a 2-day rest period after the training period before being subjected to a probe test with the removal of the platform. In the probe test, time spent in the quadrant that previously contained the hidden platform was determined as a measure of memory function. The results showed that the vehicle-treated control mice spent the longest time in the target quadrant, followed by the osmotin-treated APPsw and APP/PS1 mice; the vehicle-treated APPsw and APP/PS1 mice spent the shortest time. These results confirmed that osmotin ameliorated hippocampal spatial memory deficits in the APPsw and APP/PS1 mice (Figure 5c and Supplementary Figure S5b).

Next, the Y-maze test was performed to determine the effects of osmotin on short-term spatial memory loss in APPsw and APP1/PS1 mice. The spontaneous alternation rate from the center of the maze, which is measured as the percentage of the total number of arm entries that can be counted as nonrepetitive triplets, showed that the APPsw and APP/PS1 mice had a lower percentage of alternations than the WT control mice, indicating less working memory capacity. The percentage of alternations of the APPsw and APP/PS1 mice increased after osmotin treatment, showing that this treatment reduced the short-term spatial memory deficit in the APPsw and APP/PS1 mice (Figure 5d and Supplementary Figure S5c).

DISCUSSION

To the best of our knowledge, this is the first report describing how osmotin is involved in improving synapses, memory and cognition; reversing reductions in LTP; and diminishing the burden of Aβ by reducing cholesterol biosynthesis in APP/PS1 AD model mice. The beneficial effects of osmotin are correlated with its ability to modulate AdipoR1, activate AMPK and SIRT1 and

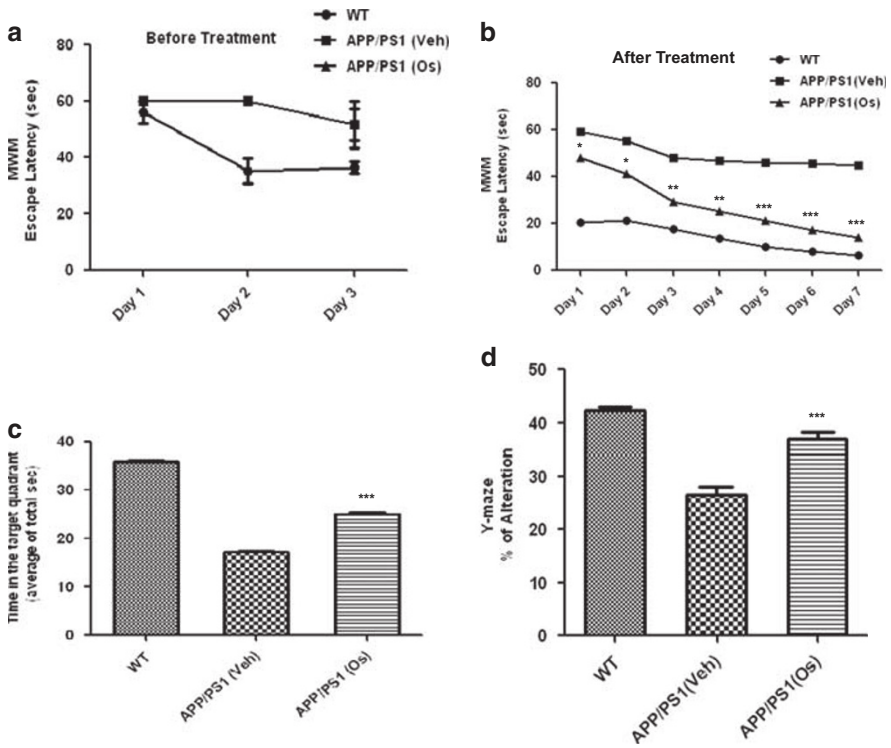

Figure 5. Osmotin (Os) diminished hippocampus-dependent spatial memory deficits in amyloid precursor protein/presenilin 1 (APP/PS1) mice. Escape latency (**a**) before osmotin treatment during the training period (submerged platform) and (**b**) after treatment in the Morris water maze (MWM) test. The escape latency of the training days was determined using repeated-measures analysis of variance (ANOVA). The data represent mean ± s.e.m. ($n = 10$/group). (**c**) The time spent in the target quadrant during the MWM probe test (platform removed) is expressed as the percentage of alternation. (**d**) The histogram shows the results of the Y-maze spontaneous alternation test performed to assess the effect of osmotin treatment on short-term memory in double-transgenic APP/PS1 Alzheimer's disease (AD) model mice. The data represent mean ± s.e.m. ($n = 10$/group). Significance: $^{*}P < 0.05$, $^{**}P < 0.01$ and $^{***}P < 0.001$.

downregulate SREBP2 to block the amyloidogenic pathway of Aβ production.

The search for new therapeutic agents for the prevention of Aβ toxicity has included agents that block the generation of Aβ, minimize its accumulation or activate the process of Aβ clearance from the entire brain or parts of the brain. Our finding that osmotin modulated AdipoR1 in both *in vitro* and *in vivo* animal models demonstrates that AdipoR1 is involved in the progression of AD. Furthermore, the osmotin-treated Adipo$^{-/-}$ mouse results fully support our current proposed mechanism of the beneficial effects of osmotin in neurodegenerative diseases such as AD. In the present study, we observed striking differences in the expression of AdipoR1 and other proteins in AD and in Adipo$^{-/-}$ mice after osmotin administration for either a short or long duration. All of these results are of clinical significance and are likely to have important implications in the pathogenesis of this disease because, presently, there are no such data. In this regard, leptin, an adipokine, has been reported to cause a reduction in Aβ via AMPK activation *in vitro* and to attenuate memory impairment in *in vivo* AD models.[19,20] Similarly, we showed that osmotin, which is a homolog of adiponectin, can potentially inhibit the amyloidogenic pathway of the Aβ-synthesizing machinery. We examined brain tissues of 5-, 9-, 12- and 16-month-old APP/PS1 mice using different techniques, such as enzyme-linked immunosorbent assay, western blotting, immunohistochemistry and immunofluorescence. Collectively, our data demonstrate that osmotin treatment can reduce the accumulation of Aβ peptides and the formation of extracellular Aβ-containing senile plaques in middle- and late-stage AD. Most importantly, we observed that osmotin treatment activated AMPK and SIRT1 both *in vitro* and *in vivo* (including both Adipo$^{-/-}$ and APP/PS1 mice) as AMPK and SIRT1 regulate each other and share downstream targets.[9] Several lines of evidence indicate that the AMPK/SIRT1 axis is involved in regulating Aβ levels in brain tissues. For example, downregulation of the expression of PP2Ca, a major AMPK phosphatase, by dietary quercetin leads to AMPK activation, reduced BACE1 expression, Aβ production and the deposition of Aβ in the brains of mice fed a high cholesterol diet.[21] AMPK directly interacts with and phosphorylates SREBP-1c and SREBP-2 to prevent their cleavage and nuclear translocation, thereby downregulating the transcription of SREBP target genes, such as those involved in cholesterol and fatty acid biosynthesis.[22] Thus, in agreement with previous studies, we found that osmotin treatment not only downregulated the abundance of total cholesterol, triglycerides, and free fatty acids in serum, but also most specifically reduced cholesterol biogenesis in the brains of Adipo$^{-/-}$ and APP/PS1 mice, both by inhibiting SREBP activity via the activation of AMPK/SIRT1 and by reducing the level of the transcription factor SREBP2. Reduced cholesterol levels in lipid rafts attenuate the activities of Aβ-synthesizing enzymes.[23–25] Thus, we found that osmotin regulated the activities of an Aβ-synthesizing enzyme (BACE1) via activated AMPK/SIRT1 and negatively regulated the SREBP2 pathway. Excess cholesterol in APP/PS1 mice induces amyloidogenesis, and drugs that inhibit cholesterol biogenesis have protective effects against amyloidogenesis.[26,27] SREBPs are key transcription factors involved in the regulation of lipid synthesis. It has been reported that SREBPs are overexpressed in APP/PS1 mice and that the overexpression of SREBP-2 in these mice results in AD pathologies.[28] The AMPKSIRT1 axis regulates lipid biosynthesis. SREBPs are substrates of AMPK, and the phosphorylation of SREBPs inhibits their lipidogenic activities.[22] SREBPs are also

substrates of SIRT1, and deacetylation by SIRT1 promotes their proteasomal degradation, thereby inhibiting their lipidogenic activities.[29] In addition, we found that osmotin treatment increased the levels of the α-secretases ADAM10 and ADAM17 that cleave the middle of the Aβ domain to preclude Aβ formation. The cleavage of APP by α-secretases generates sAPP-α, a neuroprotective extracellular fragment of APP. Osmotin treatment increased the levels of sAPP-α in the brain tissues of APP/PS1 mice, indicating that it increased α-secretase activity.

Synapses and dendritic spines, through which neurons communicate signals with each other, are especially vulnerable to AD. Cognitive decline in AD is associated with synaptic dysfunction and alterations in the number and shapes of dendritic spines, rather than with neuronal loss.[30] The ionotropic glutamate receptors AMPAR and NMDAR are contained in excitatory synapses in dendritic spines. AD brains are characterized by the loss and degeneration of dendritic spines as well as the induction of LTP. This association has been established both *in vivo* in transgenic mice and *in vitro* in neuronal cells exposed to AD-causing agents.[31,32] Considerable evidence shows that the accumulation of soluble Aβ in AD causes synaptic dysfunction, leading to AMPAR removal and the loss of dendritic spines.[33] We observed that osmotin treatment reduced Aβ levels, attenuated NMDAR loss and, most importantly, attenuated LTP in APP/PS1 mice that was correlated with cognitive and memory improvements.

Our results are consistent with the amelioration of hippocampal-dependent memory dysfunction in AD mice[34] by osmotin. Importantly, osmotin induced decreases in memory deficits, accompanied not only by a significant reduction in the amyloid burden but also by evident plaque fragmentation in the brains of transgenic mice. Similarly, our study also showed that osmotin reversed AMPA-mediated mEPSCs in *in vitro* cultured neurons, diminished the effects of Aβ and ameliorated the suppression of LTP in AD mice *in vivo*. Hence, osmotin may improve cognitive performance in transgenic mice (both APP and APP/PS1) by altering the processing of Aβ peptides, decreasing the amyloid burden, abrogating related apoptosis and neurodegeneration within the hippocampus and/or directly promoting memory formation and synaptic plasticity. Our data fully support the ability of osmotin to ameliorate AD-like pathological pathways, and they demonstrate its efficacy in reverting or preventing cognitive deterioration in APP/PS1 mice. Based on its safety and brain bioavailability, osmotin appears to be a promising drug for the prevention of AD. The outcomes of our study warrant further investigation of osmotin-like proteins or their derivatives as candidates for AD therapies based on the modification or delay of the onset of Aβ pathology.

CONFLICT OF INTEREST

The authors declare no conflict of interest.

ACKNOWLEDGMENTS

This research was supported by the Pioneer Research Center Program through the National Research Foundation of Korea funded by the Ministry of Science, ICT and Future Planning (2012-0009521).

REFERENCES

1 Cutler RG, Kelly J, Storie K, Pedersen WA, Tammara A, Hatanpaa K *et al.* Involvement of oxidative stress-induced abnormalities in ceramide and cholesterol metabolism in brain aging and Alzheimer's disease. *Proc Natl Acad Sci USA* 2004; **101**: 2070–2075.
2 Bandaru VVR, Troncoso J, Wheeler D, Pletnikova O, Wang J, Conant K *et al.* ApoE4 disrupts sterol and sphingolipid metabolism in Alzheimer's but not normal brain. *Neurobiol Aging* 2009; **30**: 591–599.
3 Xiong H, Callaghan D, Jones A, Walker DG, Lue LF, Beach TG *et al.* Cholesterol retention in Alzheimer's brain is responsible for high beta- and gamma-secretase activities and Abeta production. *Neurobiol Dis* 2008; **29**: 422–437.
4 Panchal AM, Loeper J, Cossec JC, Perruchini C, Lazar A, Pompon D *et al.* Enrichment of cholesterol in microdissected Alzheimer's disease senile plaques as assessed by mass spectrometry. *J Lipid Res* 2010; **51**: 598–605.
5 Fernandez A, Llacuna L, Fernandez-Checa JC, Colell A. Mitochondrial cholesterol loading exacerbates amyloid beta peptide-induced inflammation and neurotoxicity. *J Neurosci* 2009; **29**: 6394–6405.
6 Shepardson NE, Shankar GM, Selkoe DJ. Cholesterol level and statin use in Alzheimer disease: I. Review of epidemiological and preclinical studies. *Arch Neurol* 2011; **68**: 1239–1244.
7 Hardie DG. AMP-activated protein kinase: an energy sensor that regulates all aspects of cell functions. *Genes Dev* 2011; **25**: 1895–1908.
8 Viollet B, lantier L, Devin-Leclerc J, Hebrard JS, Amouyal C, Mounier R *et al.* Targeting the AMPK pathway for the treatment of type 2 diabetes. *Front Biosci* 2009; **14**: 3380–3400.
9 Ruderman NB, Xu XJ, Nelson L, Cacicedo JM, Saha AK, Lan F *et al.* AMPK and SIRT1: a long-standing partnership? *Am J Physiol Endocrinol Metab* 2010; **298**: E751–E760.
10 Shen Z, Liang X, Rogers CQ, Rideout D, You M. Involvement of adiponectin-SIRT1-AMPK signaling in the protective action of rosiglitazone against alcoholic fatty liver in mice. *Am J Physiol Gastrointest Liver Physiol* 2010; **298**: G364–G374.
11 Narasimhan ML, Coca MA, Jin J, Yamauchi T, Ito Y, Kadowaki T *et al.* Osmotin is a homolog of mammalian adiponectin and controls apoptosis in yeast through a homolog of mammalian adiponectin receptor. *Mol Cell* 2005; **17**: 171–180.
12 Tahir A, Gwang HY, Shahid AS, Hae YL, Myeong OK. Osmotin attenuates amyloid beta-induced memory impairment, tau phosphorylation and neurodegeneration in the mouse hippocampus. *Sci Rep* 2015; **5**: 11708.
13 Shah SA, Lee HY, Bressan RA, Yun DJ, Kim MO. Novel osmotin attenuates glutamate-induced synaptic dysfunction and neurodegeneration via the JNK/PI3K/Akt pathway in postnatal rat brain. *Cell Death Dis* 2014; **5**: e1026.
14 Naseer MI, Ullah I, Narasimhan ML, Lee HY, Bressan RA, Yoon GH *et al.* Osmotin protects against ethanol-induced apoptotic neurodegeneration in the developing rat brain. *Cell Death Dis* 2014; **5**: e115.
15 Singh NK, Bracker CA, Hasegawa PM, Handa AK, Buckel S, Hermodson MA *et al.* Characterization of osmotin. *Plant Physiol* 1987; **85**: 529–536.
16 Shah SA, Ikram U, Lee HY, Kim MO. Anthocyanins protect against ethanol-induced neuronal apoptosis via $GABA_{B1}$ receptors intracellular signaling in prenatal rat hippocampal neurons. *Mol Neurobiol* 2013; **48**: 257–269.
17 Shah SA, Gwang HY, Hyun OK, Myeong OK. Vitamin C neuroprotection against dose-dependent glutamate-induced neurodegeneration in the postnatal brain. *Neurochem Res* 2015; **40**: 875–884.
18 Meziane H, Dodart JC, Mathis C, Little S, Clemens J, Paul SM *et al.* Memory-enhancing effects of secreted forms of the beta-amyloid precursor protein in normal and amnestic mice. *Proc Natl Acad Sci USA* 1998; **95**: 12683–12688.
19 Greco SJ, Sarkar S, Johnston JM, Tezapsidis N. Leptin regulates tau phosphorylation and amyloid through AMPK in neuronal cells. *Biochem Biophys Res Commun* 2009; **380**: 98–104.
20 Grecoa SJ, Bryanb KJ, Sarkara S. Leptin reduces pathology and improves memory in a transgenic mouse model of Alzheimer's disease. *J Alzheimers Dis* 2010; **19**: 1155–1167.
21 Lu J, Wu D, Zheng Y, Hu B, Zhang Z, Shan Q *et al.* Quercetin activates AMP-activated protein kinase by reducing PP2C expression protecting old mouse brain against high cholesterol-induced neurotoxicity. *J Pathol* 2010; **222**: 199–212.
22 Li Y, Xu S, Mihaylova M, Zheng B, Hou X, Jiang B *et al.* AMPK phosphorylates and inhibits SREBP activity to attenuate hepatic steatosis and atherosclerosis in diet-induced insulin-resistant mice. *Cell Metabol* 2011; **13**: 376–388.
23 Ehehalt R, Keller P, Haass C, Thiele C, Simons K. Amyloidogenic processing of the Alzheimer beta-amyloid precursor protein depends on lipid rafts. *J Cell Biol* 2003; **160**: 113–123.
24 Kalvodova L, Kahya N, Schwille P, Ehehalt R, Verkade P, Drechsel D *et al.* Lipids as modulators of proteolytic activity of BACE: involvement of cholesterol, glycosphingolipids, and anionic phospholipids in vitro. *J Biol Chem* 2005; **280**: 36815–36823.
25 Osenkowski P, Ye W, Wang R, Wolfe MS, Selkoe DJ. Direct and potent regulation of gamma-secretase by its lipid microenvironment. *J Biol Chem* 2008; **283**: 22529–22540.
26 Refolo LM, Pappolla MA, La Francois J, Malester B, Schmidt SD, Thomas-Bryant T *et al.* A Cholesterol-lowering drug reduces β-amyloid pathology in a transgenic mouse model of Alzheimer's disease. *Neurobiol Dis* 2001; **8**: 890–899.
27 Refolo LM, Pappolla MA, Malester B, LaFrancois J, Thomas TB, Wang R *et al.* Hypercholesterolemia accelerates the Alzheimer's amyloid pathology in a transgenic mouse model. *Neurobiol Dis* 2000; **7**: 321–331.

28 Barbero-Camps E, Fernandez A, Martınez L, Fernandez-Checa JC, Colell A. APP/PS1 mice overexpressing SREBP-2 exhibit combined Aβ accumulation and tau pathology underlying Alzheimer's disease. *Hum Mol Gene* 2013; **22**: 3460–3476.
29 Walker AK, Yang F, Jiang K, Ji JY, Watts JL, Purushotham A *et al.* Conserved role of SIRT1 orthologs in fasting-dependent inhibition of the lipid/cholesterol regulator SREBP. *Genes Dev* 2010; **24**: 1403–1417.
30 Ma T, Du X, Pick JE, Sui G, Brownlee M, Klann E. Glucagon-like peptide-1 cleavage product GLP-1 (9-36) amide rescues synaptic plasticity and memory deficits in Alzheimer's disease model mice. *J Neurosci* 2012; **32**: 13701–13708.
31 Palop J, Mucke JL. Amyloid-beta-induced neuronal dysfunction in Alzheimer's disease: from synapses toward neural networks. *Nat Neurosci* 2010; **13**: 812–818.
32 Palop JJ, Chin J, Roberson ED, Wang J, Thwin MT, Bien-Ly N *et al.* Aberrant excitatory neuronal activity and compensatory remodeling of inhibitory hippocampal circuits in mouse models of Alzheimer's disease. *Neuron* 2007; **55**: 697–711.
33 Yu W, Lu B. Synapses and dendritic spines as pathogenic targets in Alzheimer's disease. *Neural Plast* 2012; **247**: 150.
34 McDonald RJ, White NM. Parallel information processing in the water maze: evidence for independent memory systems involving dorsal striatum and hippocampus. *Behav Neural Biol* 1994; **61**: 260–270.

Supplementary Information accompanies the paper on the Molecular Psychiatry website (http://www.nature.com/mp)